MARCH 14 2012

Acoustic performance of a duct loaded with identical resonators

X. Wang; C. M. Mak

J. Acoust. Soc. Am. 131, EL316–EL322 (2012)
https://doi.org/10.1121/1.3691826

Acoustic performance of a duct loaded with identical resonators

X. Wang and C. M. Mak[a)]
Department of Building Services Engineering, The Hong Kong Polytechnic University, Hung Hom, Kowloon, Hong Kong, China
09900436r@polyu.edu.hk, becmmak@polyu.edu.hk

Abstract: This paper presents a theoretical study of a duct loaded with identical side-branch resonators. The Bloch wave theory and the transfer matrix method are used to investigate wave propagation in the duct. It is found that this duct-resonator system has a unique attenuation characteristic brought about by structural periodicity. Three types of stop-bands are discussed and their bandwidths are predicted. All of the results predicted by the theory fit well with a computer simulation using a three-dimensional finite element method. Compared to a single resonator, this structure may have a potential application in broadband noise control.

PACS numbers: 43.50.Gf, 43.20.Mv [MS]
Date Received: November 30, 2011 **Date Accepted:** February 9, 2012

1. Introduction

Helmholtz resonators (hereafter resonators) are devices with a resonance peak designed to control noise in a narrow frequency range. Traditionally, resonators were regarded as lumped-parameter systems[1,2] in which the air in the neck acts as mass and the air inside its cavity acts as a spring. By considering the wave propagation inside, resonators can also be treated as distributed-parameter systems.[3,4] This model fits the experimental results better than the lumped-parameter model.

Given that a single resonator has a narrow resonance peak, combining several resonators is one possible way of obtaining a broader noise attenuation band. Some researchers have used differently tuned resonators to decrease broadband noise.[5,6] A duct loaded with identical resonators investigated by Sugimoto and Horioka[7] is found to be a new class of ultrasonic metamaterial.[8] Unlike previous theoretical discussions on the infinite periodic duct-resonator,[7,8] the present study considers a duct with a finite number of identical resonators. A modified bandwidth approximation is then proposed. A duct loaded with identical resonators exhibits an unique attenuation characteristic, which has a potential application in broadband noise control.

2. Theoretical analysis

2.1 Single resonator

As shown in Fig. 1, resonators, with neck cross sectional area S_n, neck length l_n, and cavity volume V_c, are mounted on a duct with cross sectional area S_d. Although the distributed-parameter model provides a more accurate prediction for the resonant frequency, only the lumped-parameter model is used here to give readers a clear and direct impression of the tendency of bandwidth to vary with the geometries of the resonators. Only the lossless case is considered. According to Ingard,[2] the acoustic impedance of the resonator Z_r is given as

$$Z_r = j\frac{\rho_0 l_n'}{S_n \omega}(\omega^2 - \omega_0^2), \tag{1}$$

[a)]Author to whom correspondence should be addressed.

where ρ_0 is the air density, l'_n is the effective length of the neck, and ω_0 is the resonant circular frequency (i.e., $\omega_0 = c_0\sqrt{S_n/l'_n V_c}$, c_0 is the speed of sound in the air).

2.2 A duct with resonators

As shown in Fig. 1, a typical periodic cell comprises a duct segment with a resonator attached to its left side. The diameter of the resonator neck is assumed to be negligible compared to the length of duct segment between two resonators, D. In other words, D can also be regarded as the periodic distance. The frequency range considered is well below the cut-on frequency of the duct. In the duct segment of the nth cell for $(n-1)D \le x \le nD$, the sound traveling in positive- and negative-x directions can be described with sound pressure $P_n^+(x) = C_n^+ e^{-jk[x-(n-1)D]}$ and $P_n^-(x) = C_n^- e^{jk[x-(n-1)D]}$, where C_n^+ and C_n^- are complex constants and k is the wave number. Similarly, the sound pressure in the duct segment of the next cell can be expressed as $P_{n+1}^+(x) = C_{n+1}^+ e^{-jk(x-nD)}$ and $P_{n+1}^-(x) = C_{n+1}^- e^{jk(x-nD)}$. Combining the continuity of sound pressure and volume velocity at the point $x = nD$ yields

$$\begin{bmatrix} C_{n+1}^+ \\ C_{n+1}^- \end{bmatrix} = \begin{bmatrix} (1-\xi)e^{-jkD} & -\xi e^{jkD} \\ \xi e^{-jkD} & (1+\xi)e^{jkD} \end{bmatrix} \begin{bmatrix} C_n^+ \\ C_n^- \end{bmatrix} = \mathbf{T} \begin{bmatrix} C_n^+ \\ C_n^- \end{bmatrix}, \tag{2}$$

where the 2×2-dimensional matrix $\mathbf{T}$ is the periodic transfer matrix.[9] In Eq. (2), $\xi = Z_d/2Z_r$, where Z_d/Z_r is the acoustic impedance of the duct/resonator, respectively, in which $Z_d = \rho_0 c_0/S_d$. According to the Bloch wave theory,[10] Eq. (2) can also be expressed as

$$\begin{bmatrix} C_{n+1}^+ & C_{n+1}^- \end{bmatrix}^T = e^{-jqD} \begin{bmatrix} C_n^+ & C_n^- \end{bmatrix}^T, \tag{3}$$

where the superscript T is the transposition and q is the Bloch wave number.[10] Combining Eqs. (2) and (3), the analysis of a periodic duct-resonator system boils down to an eigenvalue problem that involves finding the eigenvalue $\lambda = e^{-jqD}$ and the corresponding eigenvector $\mathbf{v} = \begin{bmatrix} v^+ & v^- \end{bmatrix}^T$ for the transfer matrix $\mathbf{T}$. Combining Eqs. (2) and (3) gives[11]

$$\cos(qD) = \cos(kD) + j\xi\sin(kD). \tag{4}$$

Generally, the eigenvalue $\lambda = e^{-jqD}$ describes the propagation property of a characteristic wave type, and that wave type, known as the Bloch wave,[10] is defined by its corresponding eigenvalue $\begin{bmatrix} v^+ & v^- \end{bmatrix}^T$, which represents the specific linear combination of positive- and negative-going planar waves. The Bloch wave number q is a complex value. In principle, there are ranges of frequencies in which q contains both a real part and an imaginary part, as $q = q_r - jq_i$. This result indicates that the energy is attenuated when waves travel through each periodic cell, and the frequency ranges are called stop-bands. In other frequency ranges, the solution only contains the real part, $q = q_r$, which indicates that there is only a phase delay when waves travel through each cell. These frequency ranges are called pass-bands.

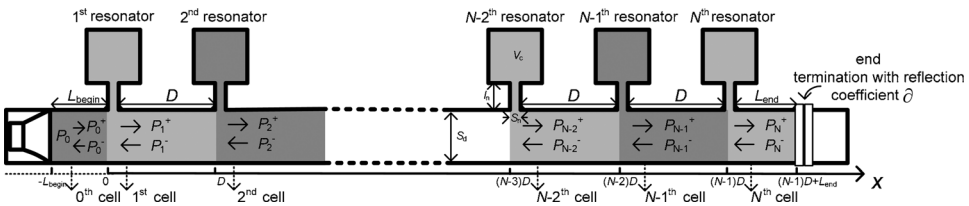

FIG. 1. A duct loaded periodically with N identical resonators.

There are two solutions of q in Eq. (4) that occur in opposite pairs: $q = \pm(q_r - jq_i)$. Assuming that $q_r > 0$ and $q_i \geq 0$, then $q = q_r - jq_i$ describes the propagation property of the "positive-going" Bloch wave, defined by the corresponding eigenvector $\mathbf{v}_1 = \begin{bmatrix} v_1^+ & v_1^- \end{bmatrix}^T$. Similarly, $q = -(q_r - jq_i)$ describes the propagation property of the "negative-going" Bloch wave, defined by the corresponding eigenvector $\mathbf{v}_2 = \begin{bmatrix} v_2^+ & v_2^- \end{bmatrix}^T$. It can be imagined that these two Bloch waves are of the same characteristic wave type but traveling in opposite directions.

Although Eq. (4) describes the frequency characteristics of the Bloch waves, it does not give an explicit expression about the position of the stop-bands, as well as their bandwidth. The theoretical prediction of the bandwidth has been proposed by Sugimoto and Horioka[7] for small resonators (compared to geometries of the duct), and this paper will expand their work to a wider applicable range by adding some modification. In general, three types of stop-bands result from either the resonance of the resonators or the Bragg reflection, or from both.[7] Using the definitions of Z_r and Z_d, Eq. (4) can be rewritten as

$$\cos(qD) = \cos(kD) + \frac{V_c k}{2S_d\left[(\omega/\omega_0)^2 - 1\right]}\sin(kD). \tag{5}$$

The first kind of stop-band (referred to as stop-band I) results from the resonance of the resonators. The stop-band is near ω_0, as $\omega/\omega_0 = 1 + \Delta$, where $|\Delta| < 1$ is assumed. To differentiate it from the other two types of stop-bands, $k_0 D \neq m\pi$ here. When the modulus of Eq. (5) is equal to unity, the approximated stop-band boundary $\Delta_{1,2}$ can be obtained as

$$\Delta_1 = \frac{V_c k_0}{4S_d}\cot\left[\frac{k_0 D}{2}(1+\Delta_1)\right] = \frac{\kappa k_0 D}{4}\left[\cot\left(\frac{k_0 D}{2}\right) - \frac{1}{\sin^2(k_0 D/2)}\frac{k_0 D}{2}\Delta_1 + \cdots\right], \tag{6}$$

$$\Delta_2 = -\frac{V_c k_0}{4S_d}\tan\left[\frac{k_0 D}{2}(1+\Delta_1)\right] = -\frac{\kappa k_0 D}{4}\left[\tan\left(\frac{k_0 D}{2}\right) + \frac{1}{\cos^2(k_0 D/2)}\frac{k_0 D}{2}\Delta_2 + \cdots\right], \tag{7}$$

where κ is the ratio of the cavity's volume to the duct's volume in a periodic cell ($\kappa = V_c/S_d D$), which is generally assumed to be smaller than unity ($\kappa < 1$). The terms contained in the square brackets of Eqs. (6) and (7) are the series expansion of the cotangent and tangent terms, respectively. The zero order corrections (the first terms in the square brackets) of Eqs. (6) and (7) give $\Delta_1 = \kappa k_0 D/4 \cdot \cot(k_0 D/2)$ and $\Delta_2 = -\kappa k_0 D/4 \cdot \tan(k_0 D/2)$, with a relative bandwidth $\Delta_{BW} = \kappa k_0 D/2 \cdot |\tan(k_0 D/2) + \cot(k_0 D/2)|$. These are obtained from Sugimoto and Horioka's examination of the issue,[7] and the bandwidth Δ_{BW} is of the order κ. However, this approximation has a significant deviation when $|\Delta| > 0.1$. A more accurate result can be obtained by considering the first order corrections (the second terms in the square brackets) of Eqs. (6) and (7), or even the higher order corrections.

The second kind of stop-band (referred to as stop-band II) is the result of the Bragg reflection, which occurs when the periodic distance becomes a multiple of a half-wavelength of sound waves ($kD = m\pi$, $m = 1, 2, \ldots$).[7] The stop-band is near $\omega_m = m\pi c_0/D$, as $\omega/\omega_m = 1 + \Delta$. To differentiate it from the third case, $\omega_m \neq \omega_0$ here. In the frequency range of stop-band II, Eq. (5) can be approximated as

$$\cos(qD) = \cos[m\pi(1+\Delta)] + \frac{\kappa m\pi(1+\Delta)/2}{\left[\omega_m(1+\Delta)/\omega_0\right]^2 - 1}\sin[m\pi(1+\Delta)] = (-1)^m\left[1 + \frac{(m\pi)^2}{2}E\right], \tag{8}$$

$$E = \frac{\kappa(1+\Delta)}{[(1+\Delta)\omega_m/\omega_0]^2 - 1}\Delta - \Delta^2, \tag{9}$$

E can be approximated as $G\Delta - \Delta^2$, where $G = \kappa/[(\omega_m/\omega_0)^2 - 1]$, which gives $\Delta_1 = 0$ and $\Delta_2 = \kappa/[(\omega_m/\omega_0)^2 - 1]$ with the relative bandwidth $\Delta_{BW} = \kappa/|(\omega_m/\omega_0)^2 - 1|$. This is derived by Sugimoto and Horioka,[7] and the bandwidth Δ_{BW} is of the order κ. Similarly, the approximation made above has a significant deviation when $|\Delta| > 0.1$. A modified approximation can be obtained by rewriting Eq. (9) as

$$E = \frac{\kappa(1+\Delta)\Delta}{2\gamma^2\Delta + \gamma^2 - 1} - \Delta^2, \tag{10}$$

where $\gamma = \omega_m/\omega_0$. In addition to $\Delta_1 = 0$, there are two other roots as

$$\Delta_{2,3} = \frac{\kappa + 1 - \gamma^2 \pm \sqrt{(\gamma^2 - 1 - \kappa)^2 + 8\kappa\gamma^2}}{4\gamma^2}. \tag{11}$$

For the stop-bands II of $\gamma < 1$, Δ_2 is in the range of $(-1,-0)$, which is the physically reasonable root. For the stop-bands II of $\gamma > 1$, the Δ_3 in the range of $(0,-1)$ should be selected.

The third case (referred to as stop-band III) results from both the resonance of the resonator and the Bragg reflection (i.e., $\omega_m = \omega_0$). In the frequency range of stop-band III, Eq. (9) can be approximated as $E = \kappa/2 - \Delta^2$, with $\Delta_{1,2} = \pm\sqrt{\kappa/2}$ and $\Delta_{BW} = \sqrt{2\kappa}$. This is obtained from Sugimoto and Horioka,[7] and the stop-band III is widened to be of the order $\sqrt{\kappa}$. As D is in this case limited to $m\pi/k_0$, the relative bandwidth Δ_{BW} is at its maximum value when $m = 1$. Similarly, the approximation has a significant deviation when $|\Delta| > 0.1$. Substituting $\omega_m/\omega_0 = 1$ into Eq. (9) gives

$$\Delta^3 + 2\Delta^2 - \kappa\Delta - \kappa = 0. \tag{12}$$

The equation above has three roots[12] as

$$\Delta_1 = -\frac{2}{3} - \frac{2}{3}\sqrt{4+3\kappa}\cos\left(\frac{\theta}{3}\right), \tag{13}$$

$$\Delta_{2,3} = -\frac{2}{3} + \frac{\sqrt{4+3\kappa}}{3}\left[\cos\left(\frac{\theta}{3}\right) \pm \sqrt{3}\sin\left(\frac{\theta}{3}\right)\right], \tag{14}$$

where $\theta = \arccos(K)$, $K = (16 - 9\kappa)/[2(4+3\kappa)^{1.5}]$. As $\Delta_1 < -1$ is physically impossible, the other two roots $\Delta_{2,3}$ are chosen. Compared to the results obtained by Sugimoto and Horioka,[7] Eq. (14) indicates that f_0 is not exactly in the middle of the stop-band.

The preceding equations describe the infinite duct-resonator structure. In a practical situation, such as a duct with N identical resonators, the influence of the beginning and end boundaries should be considered. As described above, the sound pressure in the duct segment of the nth cell can also be expressed as the combination of positive- and negative-going Bloch waves, such that

$$\begin{bmatrix} C_n^+ & C_n^- \end{bmatrix}^T = a_n\mathbf{v}_1 + b_n\mathbf{v}_2 = a_n\begin{bmatrix} v_1^+ & v_1^- \end{bmatrix}^T + b_n\begin{bmatrix} v_2^+ & v_2^- \end{bmatrix}^T, \tag{15}$$

where a_n and b_n are complex constants. By introducing Eq. (2), Eq. (15) can be expressed as

$$\begin{aligned}\begin{bmatrix} C_n^+ C_n^- \end{bmatrix}^T &= \mathbf{T}\begin{bmatrix} C_{n-1}^+ & C_{n-1}^- \end{bmatrix}^T = \mathbf{T}^2\begin{bmatrix} C_{n-2}^+ & C_{n-2}^- \end{bmatrix}^T = \cdots = \mathbf{T}^{n-1}\begin{bmatrix} C_1^+ & C_1^- \end{bmatrix}^T \\ &= a_1\mathbf{T}^{n-1}\mathbf{v}_1 + b_1\mathbf{T}^{n-1}\mathbf{v}_2 = a_1\lambda_1^{n-1}\mathbf{v}_1 + b_1\lambda_2^{n-1}\mathbf{v}_2. \end{aligned} \tag{16}$$

Combining Eqs. (15) and (16) gives $a_n = a_1\lambda_1^{n-1}$ and $b_n = b_1\lambda_2^{n-1}$. The complex constants a_1 and b_1 can be derived by considering the beginning and end boundary conditions (assumed to be anechoic, i.e., reflection coefficient $\partial = 0$), which give

$$(a_1\lambda_1^{-1}v_1^+ + b_1\lambda_2^{-1}v_2^+)e^{-jk(D-L_{begin})} + (a_1\lambda_1^{-1}v_1^- + b_1\lambda_2^{-1}v_2^-)e^{jk(D-L_{begin})} = P_0, \tag{17}$$

$$a_1\lambda_1^{N-1}v_1^- e^{jkL_{end}} + b_1\lambda_2^{N-1}v_2^- e^{jkL_{end}} = a_N v_1^- e^{jkL_{end}} + b_N v_2^- e^{jkL_{end}} = 0. \tag{18}$$

The averaged transmission loss of a duct with N resonators can be expressed as

$$\overline{TL} = \frac{20}{N}\log_{10}\left|\frac{C_0^+}{C_N^+}\right| = \frac{20}{N}\log_{10}|X|, \tag{19}$$

$$X = \frac{a_1\lambda_1^{-1}v_1^+ + b_1\lambda_2^{-1}v_2^+}{a_1\lambda_1^{N-1}v_1^+ + b_1\lambda_2^{N-1}v_2^+}. \tag{20}$$

It is interesting that although the three types of stop-bands only describe the propagation characteristic of the Bloch waves, the averaged transmission loss has a similar frequency pattern when the number of resonators is large enough (i.e., $\lim_{N\to\infty}\overline{TL} = -20\log_{10}|\lambda_1|$). Within the frequency range of stop-bands, there are $\lambda_{1,2} = e^{\mp j(q_r - jq_i)D}$. As $|\lambda_1| < 1$, when $N \to \infty$ the first term in Eq. (18) approaches zero, so $b_1 = 0$. Therefore, Eq. (19) can be rewritten as $\overline{TL} = \frac{20}{N}\log_{10}\left|\frac{a_1\lambda_1^{-1}v_1^+}{a_1\lambda_1^{N-1}v_1^+}\right| = -20\log_{10}|\lambda_1|$. Within the frequency range of pass bands, there is $\lambda_{1,2} = e^{\mp jq_rD}$. It can be imagined that $\overline{TL}$ fluctuates over the pass-band and the fluctuation decreases at the rate of $1/N$ (i.e., approaching $-20\log_{10}|\lambda_1|$).

3. Results and discussion

Figures 2 and 3 show the averaged transmission loss, $\overline{TL}$, of ducts with different numbers of resonators (N=1,2,5, ∞); the geometries are listed in the figure captions. The theoretical predictions (dotted line) in cases (N=1,2,5) are compared with the numerical simulation using the three-dimensional finite element method (solid line). The case N=1 is the common condition of a duct with a single side-branch resonator. It has been verified that in the case of $N=\infty$, $\lim_{N\to\infty}\overline{TL} = -20\log_{10}|\lambda_1|$.

The three-dimensional finite element method (called simply FEM hereafter) governed by Helmholtz equation was used. The beginning boundary was an oscillating sound pressure at magnitude of $P_0 = 1$. The end termination was set to be anechoic, with other boundaries set to be rigid. A fine mesh divided the model into more than 8000 triangular elements, with the minimum/maximum one of side-length 1.7 mm/4.8 cm observed in the duct-neck interface/duct, respectively.

Compared to geometries of the duct, the resonators used in Figs. 2 and 3 are large. To ensure the validity of the lumped model,[2] the interested frequency range is kept well below the cut-on frequency of the duct and neck. The deviation between the theoretical prediction and the FEM simulation can be observed in Figs. 2(a) and 3(a). Moreover, the theoretical predictions in Figs. 2 and 3(a) diverge at the resonance frequency in this lossless case, and there is a truncation on the peak in these figures (dotted lines). Due to the calculation error in the FEM simulation, sound pressure in the downstream duct cannot be accurately equal to zero at the resonance frequency, the

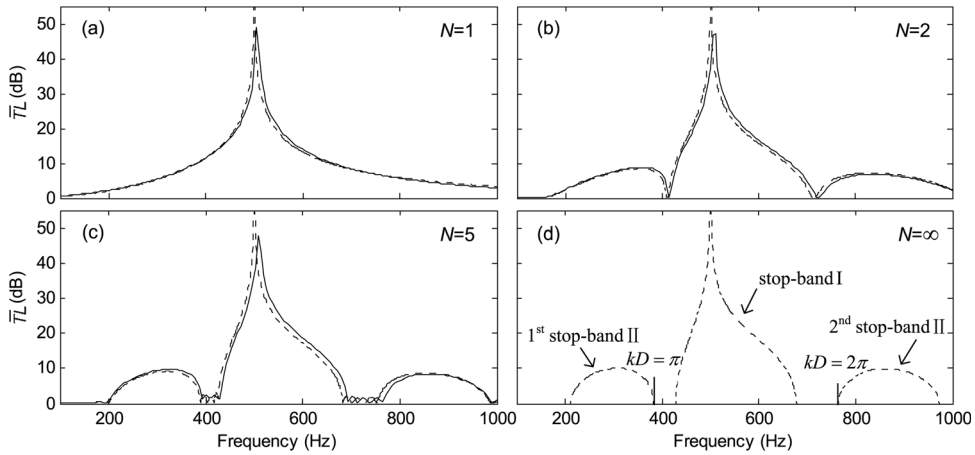

FIG. 2. The averaged transmission loss $\overline{TL}$ of the duct with N resonators (the solid lines represent the FEM simulation and the dotted lines represent the theoretical prediction). $S_n = 4\pi\,\text{cm}^2$, $l_n = 2.1\,\text{cm}$, $V_c = 136.75\pi\,\text{cm}^3$, $S_d = 12\,\text{cm}^2$, $L_{begin} = 30\,\text{cm}$, $L_{end} = 30\,\text{cm}$, $P_0 = 1\,\text{Pa}$, $\partial = 0$, and $D = 45\,\text{cm}$.

resonance peak of solid lines will not diverge. In Figs. 3(b)–3(d), the peaks of both dotted and solid lines are suppressed due to structural periodicity in the case $\omega_m = \omega_0$.

Stop-bands I and II are shown in Fig. 2(d). The Sugimoto and Horioka's approximation[7] gives stop-band I at around 280–1280 Hz ($\Delta_1 = -0.43$ and $\Delta_2 = 1.55$), and the first stop-band II at around −344–382 Hz. The modified approximation using Eqs. (6) and (7) gives stop-band I at around 430–590 Hz ($\Delta_1 = -0.14$ and $\Delta_2 = 0.18$, the consideration is up to the first order corrections) and the first stop-band II using Eq. (11) at around 210–382 Hz. Comparing the predicted stop-band I at 425–680 Hz with the first stop-band II ($kD = \pi$) at 210–380 Hz using Eq. (19) [shown in Fig. 2(d)], it is clear that the modified approximation derived from Eqs. (6), (7), and (11) shows better agreement with the theoretical prediction than that of Sugimoto and Horioka. Stop-band III is shown in Fig. 3(d). Sugimoto and Horioka's approximation gives stop-band III at 185–815 Hz, while the modified approximation derived from Eq. (14) gives stop-band III at around 240–850 Hz. Comparing the predicted stop-band III at

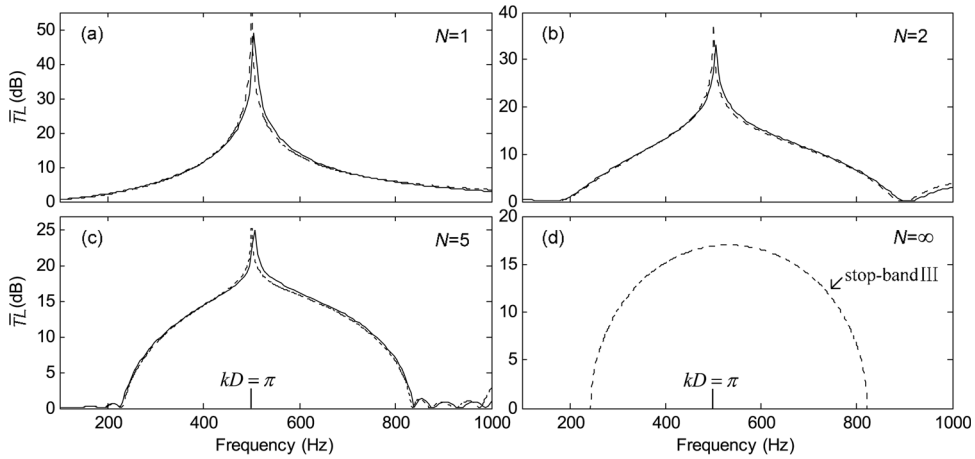

FIG. 3. The averaged transmission loss $\overline{TL}$ of the duct with N resonators (the solid lines represent the FEM simulation and the dotted lines represent the theoretical prediction). $S_n = 4\pi\,\text{cm}^2$, $l_n = 2.1\,\text{cm}$, $V_c = 136.75\pi\,\text{cm}^3$, $S_d = 12\,\text{cm}^2$, $L_{begin} = 30\,\text{cm}$, $L_{end} = 30\,\text{cm}$, $P_0 = 1\,\text{Pa}$, $\partial = 0$, and $D = 34.4\,\text{cm}$.

240–820 Hz using Eq. (19), the modified approximation has a relative error of 17%, which is less than the 24% relative error in Sugimoto and Horioka's approximation. The modified approximation makes only a slight improvement on the prediction because the modified approximation on the cosine and sine terms of Eq. (8) has a relatively low accuracy as $|\Delta| > 0.5$.

In Figs. 2 and 3, when the cases $N = 1$ are compared to other cases, there is a clear impression of the difference caused by structural periodicity. The cases $N = 2$, shown in both Figs. 2(b) and 3(b), illustrate the rudiments of the frequency attenuation caused by structural periodicity; the original pattern of frequency attenuation begins to break down under the influence of the emerging structural periodicity. In the cases $N = 5$, shown in Figs. 2(c) and 3(c), the width of the stop-bands decreases and a ripple pattern is observed beside them. That pattern disappears when $N = \infty$, as can be seen in both Figs. 2(d) and 3(d).

4. Conclusion

This paper has presented a theoretical study of a duct with identical resonators. Three types of stop-bands have been discussed, and their bandwidths have been predicted theoretically. The influence of the number of resonators has also been investigated. All of the results predicted by the theory fit well with the FEM simulation. As the case shown in Fig. 3(c), apart from the peak resulted from the resonance of a single resonator, the duct with five identical resonators provides an averaged transmission loss with a broadband around 240–820 Hz at the level of around 3–15 dB; the overall transmission loss of this system is quintupling, providing around 15–75 dB in this wide frequency range. However, to obtain such a broad stop-band, κ (usually close to 1) will be too large for those predictions derived for $\kappa \ll 1$ by Sugimoto and Horioka. It is seen that the modified approximation generally gives better prediction on the bandwidth in the cases of large κ, which helps in the duct-resonator design. In general, compared to a single resonator, a duct with several identical resonators exhibits a unique attenuation characteristic caused by structural periodicity, and may, if carefully designed, provide a much broader noise attenuation bands.

References and links

[1]J. W. S. Rayleigh, *The Theory of Sound, Volume II* (Dover, New York, 1945), Chap. 16, pp. 303–322.
[2]U. Ingard, "On the theory and design of acoustic resonators," J. Acoust. Soc. Am. **25**, 1037–1061 (1953).
[3]P. K. Tang and W. A. Sirignano, "Theory of a generalized Helmholtz resonator," J. Sound Vib. **26**, 247–262 (1973).
[4]A. Selamet, P. M. Radavich, N. S. Dickey, and J. M. Novak, "Circular concentric Helmholtz resonator," J. Acoust. Soc. Am. **101**, 41–51 (1997).
[5]A. Trochidis, "Sound transmission in a duct with an array of lined resonators," J. Vibr. Acoust. **113**, 245–249 (1991).
[6]S. H. Seo and Y. H. Kim, "Silencer design by using array resonators for low-frequency band nose reduction," J. Acoust. Soc. Am. **118**(4), 2332–2338 (2005).
[7]N. Sugimoto and T. Horioka, "Dispersion characteristics of sound waves in a tunnel with an array of Helmholtz resonators," J. Acoust. Soc. Am. **97**(3), 1446–1459 (1995).
[8]N. Fang, D. J. Xi, J. Y. Xu, M. Ambati, W. Srituravanich, C. Sun, and X. Zhang, "Ultrasonic metamaterials with negative modulus," Nature Mater. **5**, 452–456 (2006).
[9]L. Schächter, *Beam-Wave Interaction in Periodic and Quasi-Periodic Structures* (Springer, Berlin, 1997), Chap. 5, pp. 195–233.
[10]C. Kittel, *Introduction to Solid State Physics*, 6th ed. (John Wiley and Sons, Inc., New York, 1986), Chap. 8, pp. 181–216.
[11]D. C. Lay, *Linear Algebra and its Applications* (Addison Wesley, New York, 1994), Chap. 6, pp. 280–287.
[12]F. Shengjin, "A new extracting formula and a new distinguishing means on the one variable cubic equation," J. Hainan Normal Univ. (Natural Sci.) **2**(2), 91–98 (1989) (in Chinese).